PHILOSOPHICAL TRANSACTIONS OF THE ROYAL SOCIETY A MATHEMATICAL, PHYSICAL & ENGINEERING SCIENCES

The effect of strain path on material behaviour during hot rolling of FCC metals

S.B. Davenport, R.L. Higginson and C.M. Sellars

Phil. Trans. R. Soc. Lond. A 1999 **357**, 1645-1661
doi: 10.1098/rsta.1999.0394

THE ROYAL SOCIETY

The effect of strain path on material behaviour during hot rolling of FCC metals

By S. B. Davenport†, R. L. Higginson and C. M. Sellars

IMMPETUS (Institute for Microstructural and Mechanical Process Engineering), The University of Sheffield, Mappin Street, Sheffield S1 3JD, UK

Models representing material behaviour are now an essential component of the development process for rolled products. Although models based on physical parameters are being proposed, most current models employ empirical equations, which assume that the deformation can be characterized by the strain rate, temperature and the equivalent plastic strain. However, deformation in a flat product rolling pass involves a partial reversal of shear strain, and in long product and section rolling there are more complex changes in strain path in sequential passes.

This paper briefly reviews the mapping of strain paths and their effects on the micromechanics of deformation and the resulting flow stress. The influence of in-grain heterogeneity of strain is discussed in relation to the development of dislocation structures and their effects on texture evolution and subsequent recrystallization behaviour. The effects on recrystallization kinetics and resulting grain size are sufficiently large to lead to significant errors in modelling the local behaviour in multipass rolling, if strain-path effects are not considered.

Keywords: Bauschinger effects; flow stress; microstructure; microbands; texture; recrystallization

1. Introduction

All deformation processing of metals involves imparting large permanent changes of shape and, therefore, large plastic strains, which may, in general, be complex in three dimensions. The route by which the final strain state is achieved is the strain path. In practical processes, the strain rate and temperature may also change during deformation. Finite-element modelling enables each of these variables to be quantified as a function of the position of an element within the workpiece and provides a complete description of the deformation history. All aspects of the history can have important effects on the dynamic microstructural changes, which take place during the deformation, and on the static microstructural changes, which take place subsequently. In this paper, only the effects of the strain path are considered, although the magnitude of the effects of a change in strain path may in practical hot rolling processes be enhanced or diminished by strain rate and temperature changes in the deformation history.

A few years ago, McLaren & Sellars (1992) attempted to combine the outputs from a finite-element model for flat rolling with empirical equations for the kinetics of static recrystallization of type 316 stainless steel to predict the distribution of

† Present address: Delft University of Technology, Rotterdamseweg 137, 2628 AL Delft, The Netherlands.

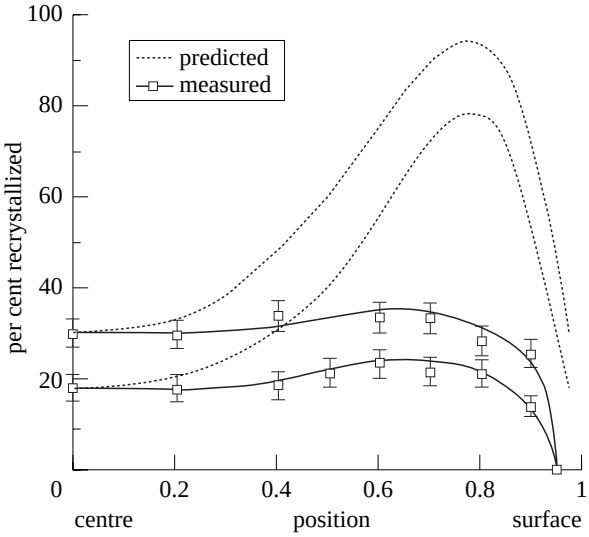

Figure 1. Predicted and measured distribution of fraction recrystallized through the thickness of a small slab of type 316 stainless steel rolled at 1000 °C and subsequently annealed for 86 or 124 s (reproduced from McLaren & Sellars 1992).

fraction recrystallized as a function of position through the thickness of a slab. The results were compared with experimental observations as shown in figure 1. It can be seen that the predicted variation is far larger than the variation observed. It was concluded that the discrepancy arose mainly from the use of equivalent strains in the equation for recrystallization kinetics, despite the fact that the sign of redundant shear strains changes during a rolling pass. It was subsequently shown (McLaren & Sellars 1993) that the way in which the final equivalent strain values were computed from the incremental strains could account for the discrepancy, but there was, then, no microstructural evidence from transmission electron microscopy to support a specific method of accumulating strain (stored energy) when changes in strain path took place.

2. Mapping the strain path

In the most general case of strains related to fixed axes, one can define three normal components of strain and six shear components of strain. For plastic deformation, the normal components $\varepsilon_{11} > \varepsilon_{22} > \varepsilon_{33}$ are not independent because there is no dilation, i.e.

$$\varepsilon_{11} + \varepsilon_{22} + \varepsilon_{33} = 0. \tag{2.1}$$

Also, the shear components are symmetric, i.e.

$$\varepsilon_{12} = \varepsilon_{21}, \qquad \varepsilon_{13} = \varepsilon_{31}, \qquad \varepsilon_{23} = \varepsilon_{32}. \tag{2.2}$$

Thus, there are only five independent strain components. Nevertheless, this is more than the three dimensions in which one can present a simple map. For graphical mapping one must, therefore, apply certain constraints.

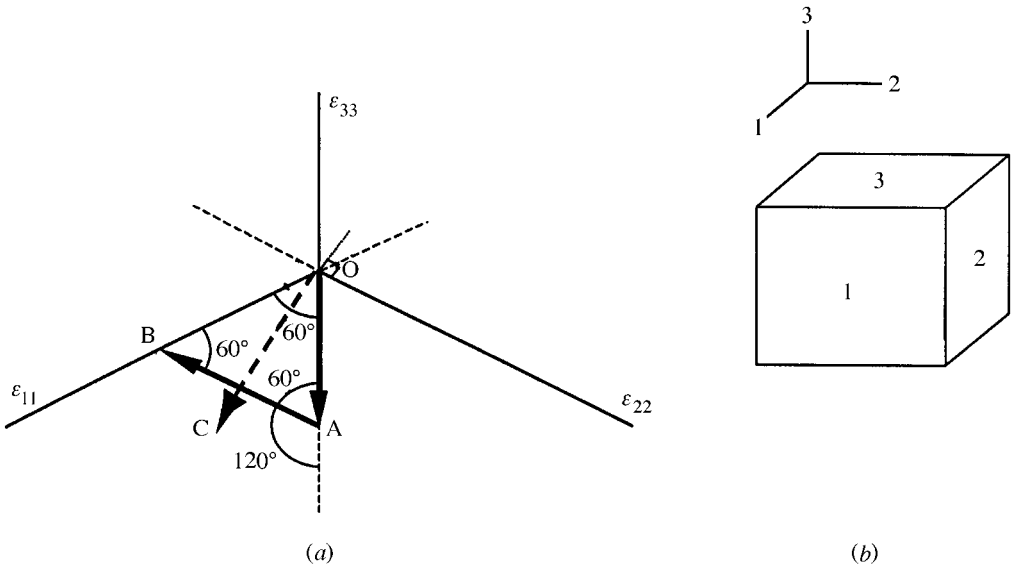

Figure 2. (*a*) Graphical representation of strain paths using axes at 120° for the normal strain components. (*b*) Cube showing faces on which sequential strains are applied to produce the vectors in (*a*).

If only the normal components are presented, then, from equation (2.1), a map in two dimensions, with the three axes at 120° to each other, can be used (Hutchinson & Davis 1983), as illustrated in figure 2, in which the positive axes are labelled.

A uniaxial compression ε_{33} on face 3 (figure 2*b*) leads to the strain vector OA in figure 2*a*, because, from equation (2.1),

$$\varepsilon_{11} = \varepsilon_{22} = -\varepsilon_{33/2}, \tag{2.3}$$

and $\cos 60 = \frac{1}{2}$.

If the specimen is then given an equal uniaxial compression on face 2, the strain path is AB, i.e. the strain path undergoes a 120° rotation. In this mapping, the gross strain OA + AB = 2 × OB, but the net strain, defined by the initial and final positions in strain space is $\overline{\mathbf{OA}} + \overline{\mathbf{AB}} = \overline{\mathbf{OB}}$, where $\overline{\mathbf{OB}}$ is equivalent to a single uniaxial tension applied to face 1. In contrast, if an initial plane-strain compression is applied to face 3, in a channel die with $\varepsilon_{22} = 0$, then the strain path is **OC**. Applying a second plane-strain compression on face 1, with $\varepsilon_{22} = 0$, then reverses the path along **CO**. This is a 180° rotation of the strain path (comparable with a total reversal of the direction of twist in torsion). Other systematic changes in strain path can be obtained by different combinations of uniaxial and plane-strain compression, so this representation is useful when ε_{11}, ε_{22} and ε_{33} are the principal strains, which do not change orientation in space as a function of strain. In the rolling of rods, alternative passes may be considered as imposing compressive strains in the 3 and 2 directions. Also, for beams, alternative passes may operate on the thickness of the flange and on the edge of the flange. However, in addition to these normal strains there are shear strains, so the orientation of the principal strains is changed. In this general case of an element in which the orientation of the principal axes changes with strain, a further orientation diagram is required to describe the change in strain path, which makes interpretation of observed microstructures difficult.

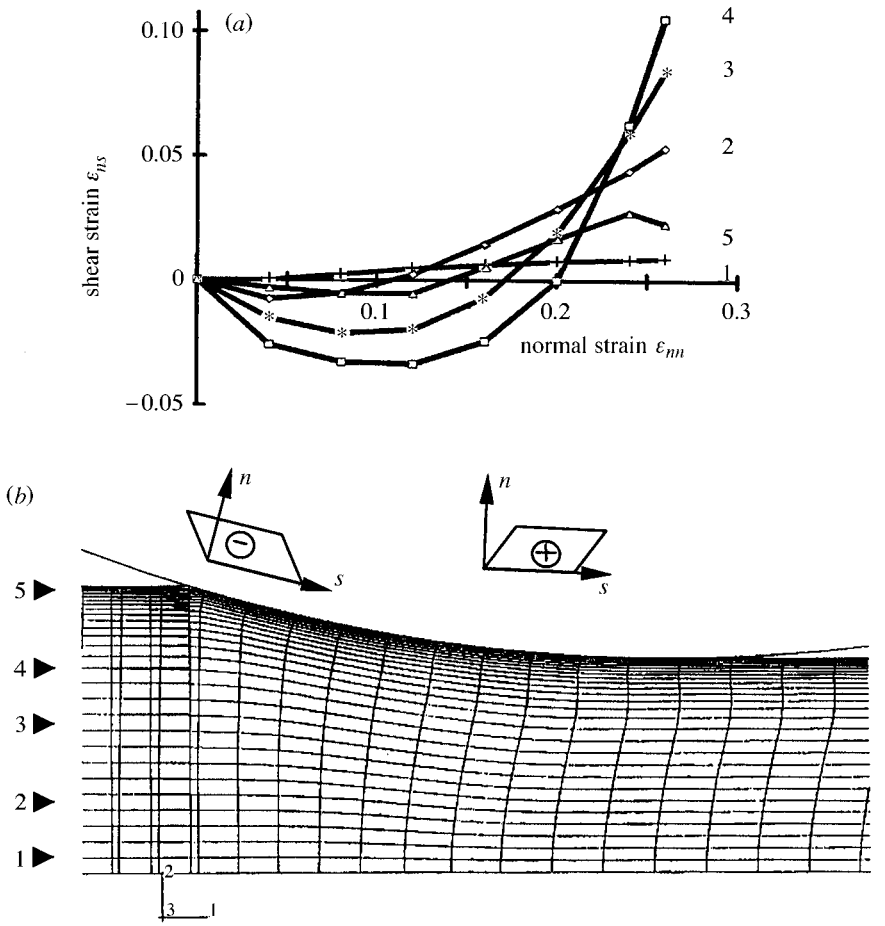

Figure 3. (*a*) Shear strain as a function of normal strain at different positions within the thickness of a slab subject to plane-strain rolling. (*b*) Geometry of rolling, showing the streamlines and the change in shape of each finite element during the pass (Mukhopadhyay 1998).

Rolling of flat products approximates to plane-strain conditions, $\varepsilon_{22} = 0$, i.e. the longitudinal and thickness strains are related as

$$\varepsilon_{11} = -\varepsilon_{33}. \tag{2.4}$$

In this case, the only change in strain path arises from the value of the shear-strain component. The mapping of the strain path is, then, best presented in terms of the shear strain as a function of the normal strain (as shown in figure 3*a*). It should be noted that the lines in this figure are obtained by integrating the normal and shear components of strain rate as a function of time during deformation, so that a vertical line does not necessarily represent the strain state at a constant time, except at entry and exit. In fact, figure 3*a* shows the normal strain ε_{nn} related to the normal to the streamline, and ε_{ns} shows the shear strain related to the same axes, which, as shown in figure 3*b*, rotate with respect to the global geometric axes of the longitudinal and through-thickness directions. At entry and exit the orientation of the axes is identical, but, during the roll pass, the local axes provide a better

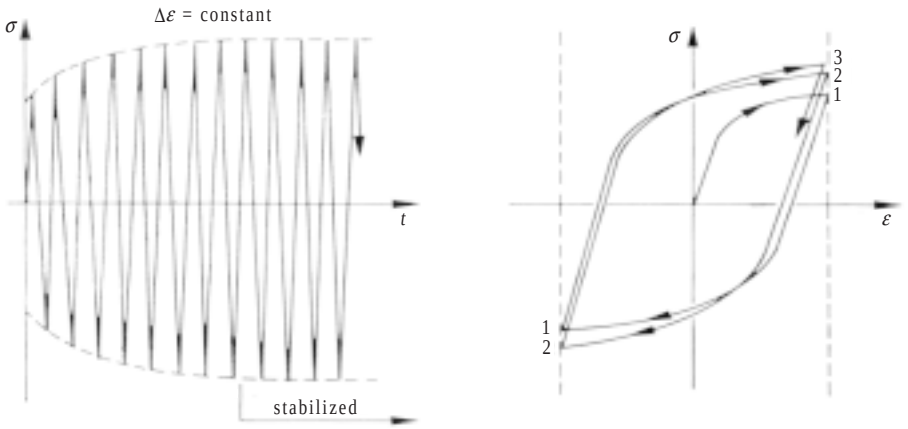

Figure 4. The evolution of the stress–strain curve during fatigue under cyclic tension–compression, showing cyclic hardening to steady state (reproduced from Lemaitre & Chaboche 1994).

description of the strain path in relation to microstructural evolution (Ponter *et al.* 1993). From figure 3*a* it can be seen that there is a shear-strain contribution at all thickness positions away from the centreline. This contribution increases to the streamline at about 0.8 of the half-thickness from the centreline, and then the shear strain decreases. This decrease is influenced in the present case by the roll chilling of the surface layers, which increases the flow stress of the type 316 stainless steel used in the computation, and so results in maximum shear inside the material at position 4. Using the local axes related to the orientation of the streamlines, it is apparent that the sense of the shear strain changes at some point within the pass, so that the net value is very different from the gross value defined by the sum of the squares of the incremental strain components. This point is of importance in relation to the development of lattice curvature and to the observed static microstructural changes after rolling (figure 1).

3. Stress response

The response of the plastic flow stress of a material to a change in strain path is clearly of direct importance in the constitutive equations used as inputs to finite-element models, if the correct tractions are to be computed. However, for computation of microstructural evolution, the evolution of dislocation density and its distribution, which lead to the stress response, must also be defined.

On a macroscopic scale, the simplest case to consider is a complete reversal of strain path, e.g. tension to compression, as is typically appropriate to fatigue deformation. The stress response of an initially annealed material is then of the form illustrated in figure 4. The initial (small) plastic strain in tension leads to work hardening, which, on reversal of the strain direction to compression, results in a lower plastic yield stress than the final plastic flow stress in tension (the Bauschinger effect, see Bauschinger (1881)). With further cycles, there is cyclic hardening to a steady-state value, which then remains constant.

This change in flow stress can be represented by the behaviour of the plastic yield surface in stress space, illustrated in figure 5. The plastic deformation can result in

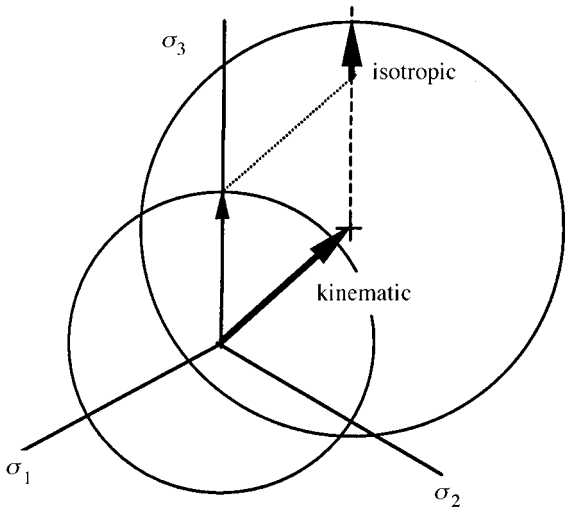

Figure 5. Schematic of the plastic yield stress surface in stress space showing isotropic and kinematic hardening effects.

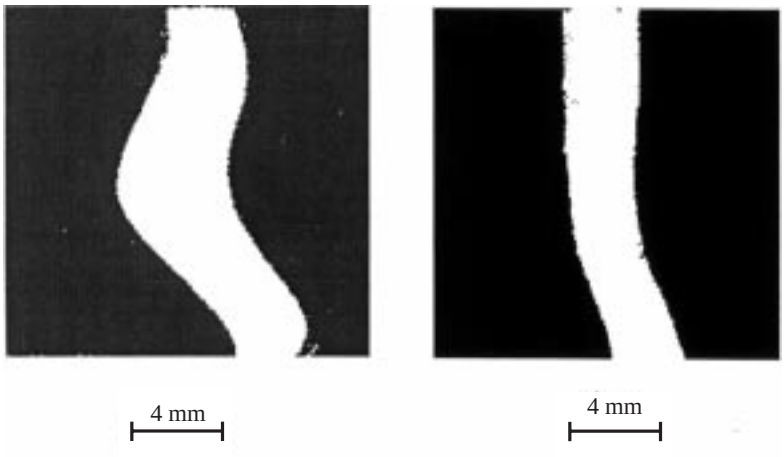

Figure 6. Experimental observation of the shape of pins inserted through the thickness of small slabs subject to two-pass rolling of 30% and 20% reduction (*a*) in forward–forward rolling, and (*b*) in forward–reverse rolling (Higginson & Sellars 1997).

two effects, the first is 'isotropic hardening', which results in an increase in radius of the yield surface with no dependence on direction of straining. As discussed later, this can be considered to result from an increase in dislocation density, without any dependence on the distribution of dislocations and Burgers vectors. The second effect is 'kinematic hardening', which is represented by a shift in the centre of the yield surface, without any change in radius. Under fatigue conditions, when steady state is obtained, the entire hardening can be considered to be kinematic and the effect of strain path can then be modelled with reasonable accuracy by considering a 'memory effect' from the initial deformation, represented as a scalar quantity (Wang & Brown 1994). Under thermomechanical processing conditions, steady state is never

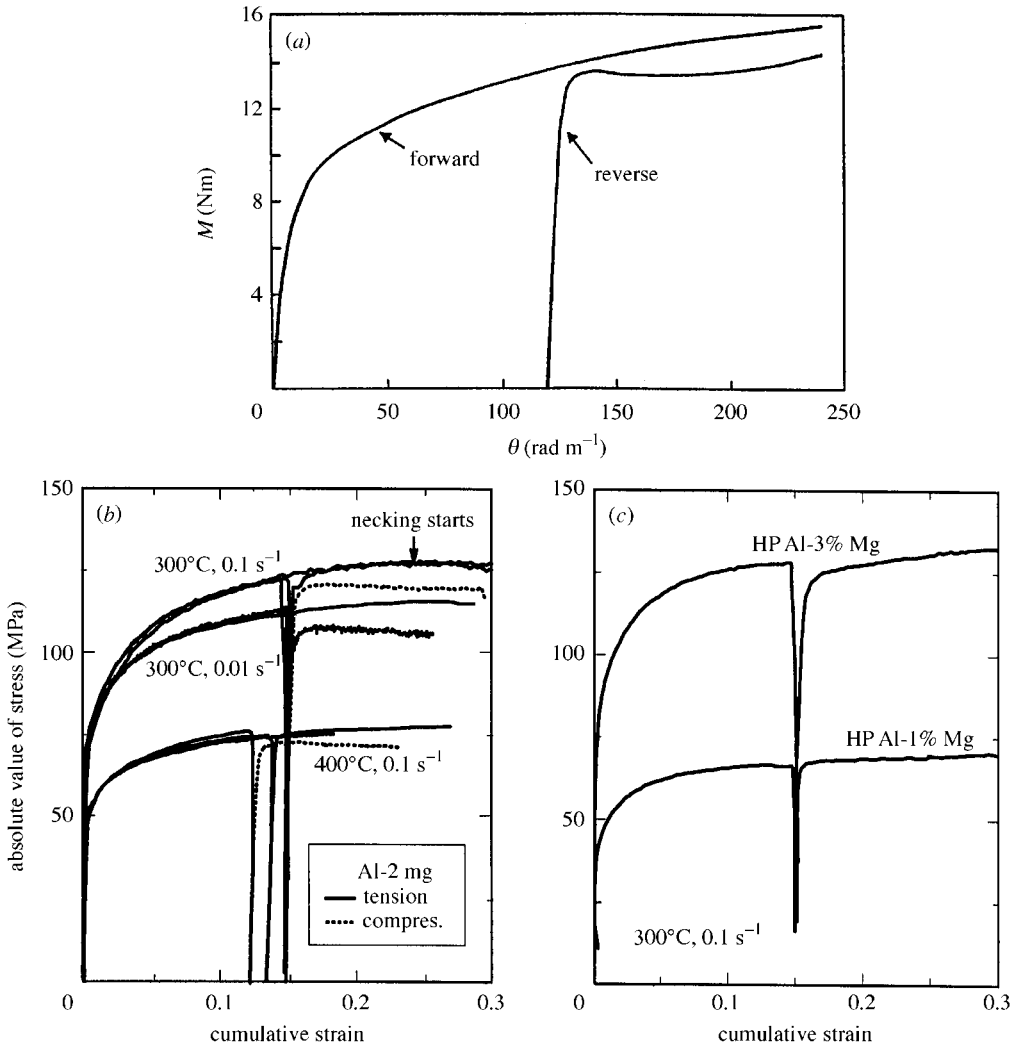

Figure 7. Stress-strain curves arising from a reversal of straining direction. (*a*) AA1050 aluminium in torsion at room temperature (reproduced from Cowan *et al*. 1995). (*b*) Commercial-purity Al–Mg alloys in tension–tension and tension–compression at 300 and 400 °C. (*c*) High-purity alloys with reversed straining (reproduced from Sellars & Zhu 1998).

achieved because the normal strains do not reverse. However, in rolling, as indicated in figure 6, the shear strains may either be additive in sequential passes in tandem mill rolling (forward–forward) or subtractive in reversing mill rolling (forward–reverse). In figure 6*a*, the additive effect of the local shears in each pass (illustrated in figure 3) results in increased pin curvature. In figure 6*b*, the reversal has almost eliminated the net shear. If recrystallization does not take place between passes, the microstructural evolution may, therefore, differ for these different strain paths and lead to different contributions to kinematic hardening in multipass rolling.

If the direction of the normal strains is changed in sequential deformations, as illustrated in figure 2*a*, the stress response depends on the angular change between the

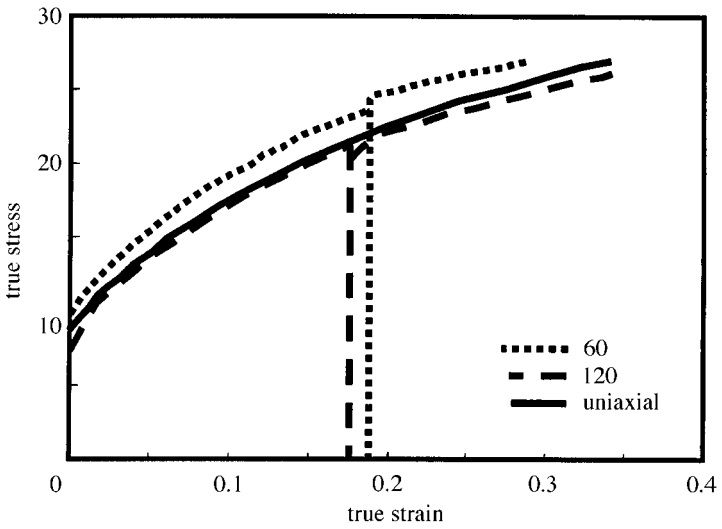

Figure 8. Stress–strain curves for Cu deformed in compression at room temperature with changes of 60 and 120° in strain paths (Poths 1998).

first and second strains. For a reversal of strain direction (180° change), Bauschinger softening with its associated reduction in work hardening rate has been observed both under cold (Stout & Rollett 1990; Embury *et al*. 1992; Cowan *et al*. 1995; Zhang *et al*. 1997; and see, for example, figure 7*a*) and hot deformation conditions (Sellars & Zhu 1998; also see figure 7*b*, *c*). However, as illustrated in figure 7*b*, *c*, the nature and magnitude of the softening differs widely in alloys of different solute or second-phase particle content.

For lower changes in orientation of sequential strains in strain space (figure 8), 'cross hardening' may be observed when the change is less than some critical value (Wang & Brown 1994; Poths 1998), e.g. increment in stress after the first strain in the curve for 60° change in figure 8, or 'Bauschinger softening' may be observed when the change is greater than the critical value, e.g. decrease in flow stress after the first strain in the curve for 120° change in figure 8.

4. Microstructural effects

In order to interpret the different effects of strain-path changes, it is important to recognize that the dislocation structures in materials deformed by a single deformation with a relatively simple strain path can differ widely, e.g. for a slightly off-centre element in plane-strain rolling in which there is compression and shear. This is shown schematically in figure 9, in which the deformation of a small volume within a single grain in an isotropic polycrystalline material is represented.

In figure 9*a*, the strain is homogeneous and equal to the strain of the whole finite element. This is the situation assumed by Taylor (1938), which leads to a homogeneous rotation of the crystal lattice within the grain. In 'ideal plastic' deformation, all the dislocations producing the plastic strain would have totally transversed the volume, leading to no hardening. For the Taylor model, the dislocations transversing the volume at the end of deformation would be of five different Burgers vectors, with equal numbers of positive and negative dislocations homogeneously distributed as

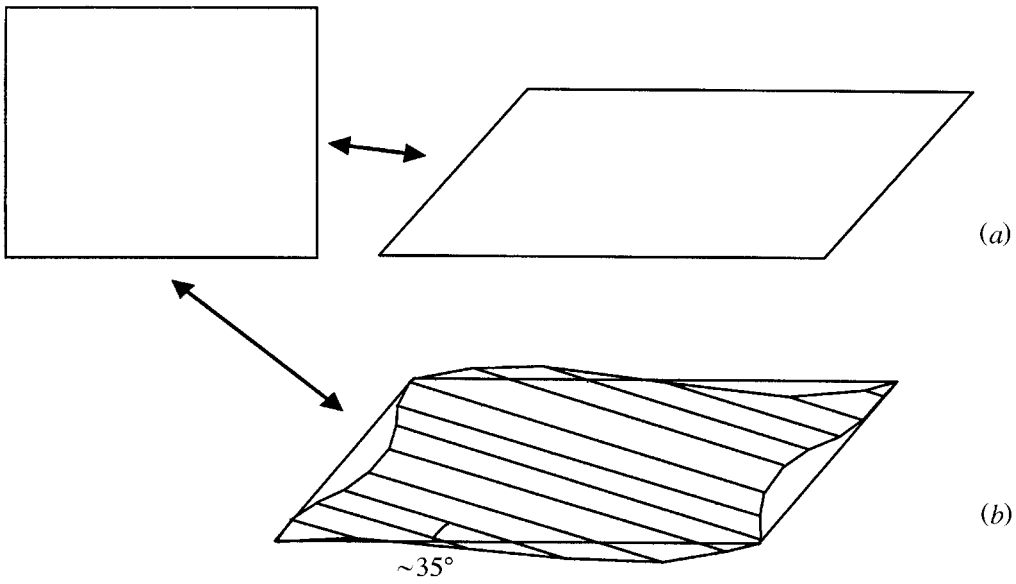

Figure 9. Schematic of deformation within a grain in an isotropic polycrystal showing (*a*) the ideal situation envisaged by Taylor, and (*b*) heterogeneity of deformation leading to lattice misorientations (curvature) with the grain.

a three-dimensional network throughout the volume. The specific Burgers vectors depend on the grain orientation, but for a random polycrystal, increasing strain in this situation leads to an increase in dislocation density trapped in transit at any strain, resulting in isotropic hardening. In practice, the dislocations are not homogeneously distributed, but many are clustered in equiaxed cell boundaries after cold rolling, or in equiaxed subgrain boundaries after hot rolling (Humphreys & Hatherley 1995). These boundaries have small, less than or equal to 2°, misorientations across them, and, for practical purposes, the structure may still be considered to result only in isotropic hardening in a randomly oriented polycrystalline metal. Thus, if the strain is reversed to regain the original shape of the volume, the major consequence will be an increase in isotropic hardening after a short transient Bauschinger effect as dislocations reverse their direction of glide. It has been proposed that these dislocation structures also have a 'polarity', so that, upon strain reversal, the cell boundaries begin to untangle (Stout & Rollett 1990; Hasegawa *et al*. 1986). However, as discussed below, it is considered that this interpretation may relate to boundaries of geometrically necessary dislocations arising from lattice curvature, rather than from the statistically stored subgrain walls in homogeneously deformed grains.

If large strains are imparted, grain rotations result in the development of crystallographic texture (preferred orientation). The homogeneous deformation in figure 9*a* is the basis for the 'full-constraint' model for texture development proposed by Taylor (1938) and developed by Bishop & Hill (1951). The effects of strain path on texture are considered in the next section.

In figure 9*b*, the local strains between microbands (i.e. in cell blocks, see Hansen (1996)) inside the volume of the grain differ, leading to internal misorientations (or lattice curvature) within the grain, even though the average strain is identical to that in figure 9*a*. This type of microstructure has been extensively studied after cold

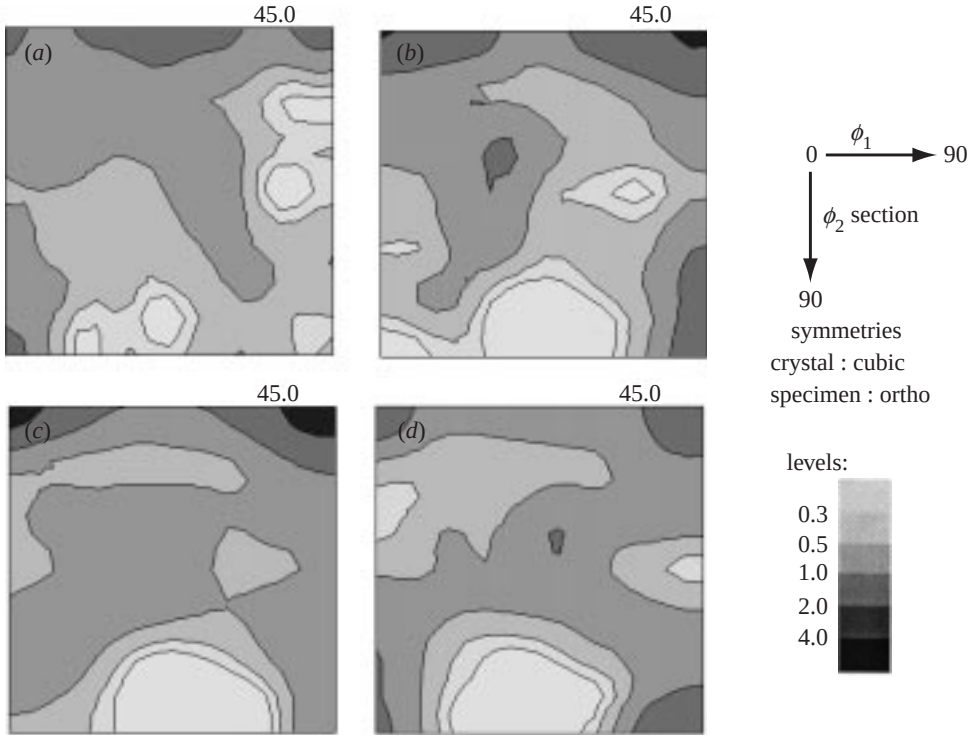

Figure 10. Constant sections ($\phi_2 = 45°$) through orientation space viewed in the 1 direction for Al–1%Mn: (*a*) original texture; (*b*) after strain OA = −0.2 (figure 2); (*c*) after strain AB = −0.2 (figure 2); and (*d*) after strain BO = −0.2 (figure 2).

rolling aluminium (Bay *et al*. 1992; Hansen 1996), and, to a more limited extent, after hot working commercial-purity aluminium magnesium alloys (Zhu & Sellars 1996; Duly *et al*. 1996), and after warm rolling (BCC) interstitial-free (IF) steels (Barnett & Jonas 1997; Akbari *et al*. 1997). What appear to be the same microstructural features have been variously referred to as 'dense dislocation walls' (Bay *et al*. 1992; Hansen 1996), 'microbands' (Zhu & Sellars 1996; Duly *et al*. 1996), and 'in-grain shear bands' (Barnett & Jonas 1997). In all cases, the features tend to be preferentially oriented at about 35° to the rolling plane. The reason for this preferred angle for macroscopic shear bands has been discussed in crystallographic terms by Dillamore *et al*. (1979), yet it appears that the angle is preferred in grains of different orientation and even in both FCC and BCC structures. The bands may, therefore, be essentially non-crystallographic, but have a preferred geometrical orientation related to the strain path. Their mechanism of formation is not yet clear, but they result in a high density of 'geometrically necessary' dislocations to accommodate the relatively large 10° misorientations between the bands. These dislocation structures appear to be superimposed on the isotropic structures in figure 9*a*. However, the increase in flow stress produced by the high density of geometrically necessary dislocations may be small, e.g. the small differences in the initial stress–strain curves for CP Al–1%Mg alloy, in which microbands are prominent, and the high-purity alloy, in which they

are not (Sellars & Zhu 1998). Texture development for these deformation structures will not be as sharp as for homogeneous strain because of the in-grain curvatures. It may, therefore, be considered as developing with 'relaxed constraints', as proposed by Canova *et al*. (1984).

When the straining direction is reversed for these structures, it appears that the misorientation between bands (lattice curvature) progressively decreases (Zhu & Sellars 1996), so that when the original shape is regained, the geometrically necessary dislocations have been removed and the structure is similar to that on reversal in figure 9*a*. This has been proposed as the reason for the large-strain Bauschinger softening for the commercial alloy in figure 7*b* compared with the almost negligible effect in the high-purity alloys (figure 7*c*).

It is attractive (but probably too simplistic) to consider that the geometrically necessary dislocations, arising from heterogeneity of local strains within grains, lead to the kinematic hardening component. Thus, when the strain path is reversed, as shown in figure 7, or nearly reversed (e.g. 120° rotation in strain space), as shown in figure 8, the mobile dislocations do not have increased interaction with the geometrically necessary dislocations, whose density decreases with increases in the reversed strain, leading to a reduced work hardening rate and large-strain Bauschinger softening. Conversely, after a smaller change in strain path (e.g. 60° rotation in strain space) as shown in figure 8, the mobile dislocations interact more strongly with the geometrically necessary dislocations from the first strain, leading to initial 'cross hardening'. Much further research is required to establish a full relationship between dislocation structures and the effect of changes in strain path on flow stress, but the above simple concept provides a link between the macroscopic and microscopic consequences in terms of flow stress and subsequent static recrystallization behaviour discussed later.

5. Deformation-texture effects

The nature of the texture depends on the specific path of a unidirectional deformation, with the rate of change of the orientation of any particular grain being proportional to the current rate of slip on its active slip systems (Takeshita *et al*. 1988).

Taylor related the flow stress (σ) of a polycrystal to the resolved shear stress for slip of a single crystal (τ) as

$$\sigma = M\tau, \tag{5.1}$$

where M is effectively an orientation factor averaged over all the grain orientations in the polycrystal. For random orientations in FCC metals, $M = 3.1$, but, as crystallographic texture develops, the value of M changes. This results in kinematic hardening (or softening) of polycrystalline metals as texture develops (Shrivistava *et al*. 1982).

There has been little experimental work on the influence of changes in strain path on deformation textures. The effect of reversing the strain path was first examined by Rollett *et al*. (1988), who concluded that the texture is not reversible. However, more recent work by Vatne *et al*. (1996) led to the conclusion that the texture is essentially fully reversible. This conclusion is more consistent with the Taylor theory and with limited results on changing the strain path. Three sequential orthogonal

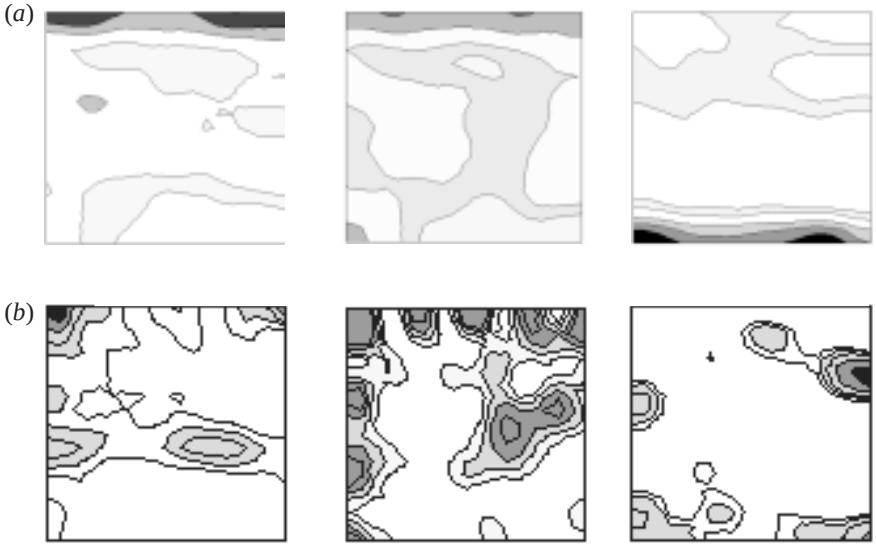

Figure 11. Constant sections (45°) through orientation space for Al–1%Mn rolled 50% reduction at 400 °C. (*a*) Experimental observation; (*b*) computed texture for (i) centreline, (ii) 0.8 of half-thickness, (iii) near-surface (Pinna *et al*. 1998).

strains have been carried out, as shown by the vectors for uniaxial compression in figure 2, with strains of −0.2. Sections of orientation distribution functions (ODFs) at constant $\phi_2 = 45°$ viewed in the 1 direction are given in figure 10. Figure 10*a* shows the original near-random texture. Figure 10*b*, *c* shows the textures at points A and B in figure 2, and figure 10*d* shows the final texture when the original shape has been regenerated by a strain BO. It can be seen that although there is a decrease in the intensity of the texture components compared with the intensity at points A and B, the original texture is not regenerated. Further research is clearly required to understand and model texture development in section rolling, where changes in orientation of the normal strains occur between passes.

In flat product rolling, the deformation textures developed at different positions through the thickness have been widely studied (Sakai *et al*. 1987; Daaland *et al*. 1992; Raabe 1995*a*, *b*). These all show the important effect of the partly reversed shear strains superimposed on the plane-strain compression at positions away from the centreline, as illustrated, for example, by the experimental ODFs in figure 11*a*. By combining the outputs of a finite-element model for rolling of an isotropic polycrystal, which shows the change in strain path as a function of element position in the thickness (illustrated in figure 3), with the full-constraint Taylor model for development of deformation texture, the textures shown in figure 11*b* have been predicted (Pinna *et al*. 1998). It is clear that the model captures only some essential consequences of the different strain paths, and, surprisingly, the best prediction is for the surface, but in common with most other texture models, it overpredicts the strength of the texture components. This could arise partly from the presence of in-grain curvatures and microbands (illustrated in figure 9*b*), but further experimental work and model development is required to establish this.

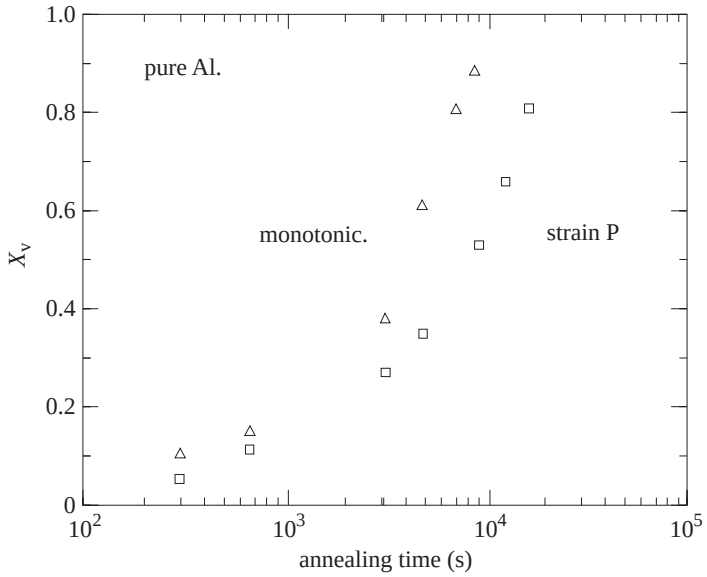

Figure 12. Comparison of recrystallization kinetics of pure aluminium deformed in channel die compression at room temperature to the same equivalent strain, monotonically and with a path change of 180° in strain space (reproduced from Embury *et al*. 1992).

6. Effects on static recrystallization

Research on the effects of changes in strain path during deformation on the subsequent static recrystallization behaviour is still very limited. The results of Embury *et al*. (1992) on pure aluminium using room-temperature channel die compression show a significant retardation of recrystallization for a 180° change in strain path compared with unidirectional deformation to the same equivalent strain (figure 12). The time for 50% recrystallization ($t_{0.5}$) is increased by a factor of about 2. Increases in $t_{0.5}$ by a factor of 3–4 have been reported after reversed torsion (180° rotation in strain space), compared with unidirectional torsion of AA1050 aluminium at room temperature (Cowan *et al*. 1995). Equivalent effects of reversed strain path have also been observed after room-temperature deformation of copper (Lindh *et al*. 1993). Less severe changes in path, e.g. 120°, have a smaller effect (Poths 1998), and 90° or 60° changes may have negligible effect (Cowan *et al*. 1995; Poths 1998). Humphreys & Hatherley (1995) have interpreted these effects in terms of the changes in flow stress or stored energy produced by change of strain path. However, the recrystallized grain size is also increased when the recrystallization kinetics are retarded (Cowan *et al*. 1995; Poths 1998) indicating that the distribution of dislocations, which influences nucleation, as well as the total dislocation density, is important. This view is supported by observations of static recrystallization after hot deformation of aluminium–magnesium alloys subject to unidirectional compression or compression plus tension to the same equivalent strain of about 0.3 (Zhu & Sellars 1996; Sellars & Zhu 1998). For the high-purity alloys in which little Bauschinger effect was observed (figure 7*c*), the retardation in $t_{0.5}$ was about a factor of 5, with little increase in grain size. In contrast, in the commercial alloy (figure 7*b*), in which the Bauschinger effect was attributed to the development and disappearance of microbanding, the retardation

in $t_{0.5}$ was about a factor of 100, with an increase in recrystallized grain size by a factor of 6. It is, therefore, proposed that only small strain-path effects arise from the forest dislocation density and equiaxed (statistically stored) low misorientation subgrain boundaries, and that large effects arise from geometrically necessary dislocations associated with lattice curvature and microband formation. Further research is required to substantiate this interpretation, which has important implications for modelling the behaviour of different alloys.

7. Concluding remarks

Representing changes in strain path for general deformations is difficult, but for rolling, mapping of the major changes is possible. During a flat rolling pass, path differences arise mainly from the superposition of reversing shear strains on the plane-strain compression deformation. For rod, bar and section rolling, more complex changes in strain path can arise from the change in direction of straining between passes on the whole cross-section or in local elements. Basic studies have shown that a reversal of strain path may result in Bauschinger softening to different extents, depending on the nature of the dislocation structures generated by deformation. In-grain lattice curvatures occurring in specific directions, and the geometrically necessary dislocations associated with them, appear to be particularly significant in this respect and may dominate the 'kinematic softening' by reversed straining and 'cross hardening' produced by smaller changes in strain path. The detailed mechanisms by which this occurs are not yet clear, but the consequences on the kinetics of subsequent static recrystallization and recrystallized grain sizes may be of major importance in modelling multipass rolling. They are clearly of sufficient magnitude to account for discrepancies between predictions made without taking account of strain-path changes and observations. In multipass rolling, the effect on computation of local stress of an erroneous estimate of the fraction of recrystallized structure entering a pass can be much larger than neglect of the relatively small direct effects of changes in strain path on the flow stress of unrecrystallized material. Further research involving closer simulation of strain-path changes in rolling, e.g. by combined compression torsion tests, and subsequent quantitative characterization of the deformed structures, e.g. by EBSP, is clearly essential for developing improved physically based models of industrial rolling processes. Such work is currently being undertaken at IMMPETUS.

The authors are grateful to the Engineering and Physical Science Research Council (EPSRC) for financial support of research by S.B.D. and R.L.H.

References

Akbari, G. H., Sellars, C. M. & Whiteman, J. A. 1997 Microstructural development during warm rolling of an IF steel. *Acta Mater.* **45**, 5047–5058.

Barnett, M. R. & Jonas, J. J. 1997 Influence of ferrite rolling temperature on microstructure and texture in deformed low C and IF steels. *Trans. Iron Steel Inst. Jap.* **37**, 697–705.

Bauschinger, J. 1881 *Zivilinger* **27**, 289–347.

Bay, B., Hansen, N., Hughes, D. A. & Kuhlmann-Wilsdorf, D. 1992 Overview no. 96—evolution of FCC deformation structures in polyslip. *Acta Metall. Mater.* **40**, 205–219.

Bishop, J. F. W. & Hill, R. 1951 A theory of the plastic distortion of a polycrystalline aggregate under combined stresses. *Phil. Mag.* **42**, 414–427.

Canova, G. R., Kocks, U. F. & Jonas, J. J. 1984 Theory of torsion texture development. *Acta Metall.* **32**, 211–226.

Cowan, J. R., Higginson, R. L., Hutchinson, W. B. & Bate, P. S. 1995 Recrystallisation following non-proportional straining in aluminium. *Mater. Sci. Tech.* **11**, 1104–1109.

Daaland, O., Maurice, C., Driver, J., Raynaud, G. M., Lequeu, P., Strid, J. & Nes, E. 1992 Evolution of microstructure and texture during hot rolling and annealing of aluminium alloy AA 3004. In *Proc. 3rd Int. Conf. on Aluminium Alloys (ICAA3)* (ed. L. Arnberg, O. Lohne, E. Nes & N. Ryum), vol. II, pp. 297–304. Trondheim, Norway: Norwegian Institute of Technology.

Dillamore, I. L., Roberts, J. G. & Bush, A. C. 1979 Occurrence of shear bonds in heavily rolled cubic metals. *Mater. Sci.* **13**, 73–77.

Duly, D., Baxter, G. J., Shercliff, H. R., Whiteman, J. A., Sellars, C. M. & Ashby, M. F. 1996 Microstructure and local crystallographic evolution in an Al–1wt%Mg alloy deformed at intermediate temperature and high strain rate. *Acta Mater.* **44**, 2947–2962.

Embury, J. D., Poole, W. J. & Koken, E. 1992 Some views on the influence of strain path on recrystallisation. *Scr. Metall. Mater.* **27**, 1465–1470.

Hansen, N. 1996 Microstructure and texture evolution during thermomechanical processing. In *Aluminium alloys for packaging II*, pp. 11–26. Warrendale, PA: The Minerals, Metals and Materials Society.

Hasegawa, T., Yakou, T. & Kocks, U. F. 1986 Forward and reverse re-arrangements of dislocations in tangled walls. *Mater. Sci. Engng* **81**, 189–199.

Higginson, B. L. & Sellars, C. M. 1997 The effect of strain path during hot rolling on the recrystallisation kinetics of 316 stainless steel. In *Proc. Thermec 97 Int. Conf. on Thermomechanical processing of Steels and other Materials*, vol. 1, pp. 779–785. Warrendale, PA: The Minerals, Metals and Materials Society.

Humphreys, F. J. & Hatherley, M. 1995 *Recrystallisation and related annealing phenomena.* Oxford: Pergamon.

Hutchinson, W. B. & Davis, T. 1983 The effect of strain path changes on the plastic flow properties of steel. In *Proc. 4th Int. Conf. On Mechanical Behaviour of Materials* (ed. J. Carlsson & N. G. Ohlson), pp. 1227–1236. Oxford: Pergamon.

Lemaitre, J. & Chaboche, J. L. 1994 *Mechanics of solid materials.* Cambridge University Press.

Lindh, E., Hutchinson, W. B. & Ueyama, S. 1993 Effect of redundant deformation on recrystallisation behaviour of copper. *Scr. Metall. Mater.* **29**, 347–352.

McLaren, A. J. & Sellars, C. M. 1992 Modelling distribution of microstructure during hot rolling of stainless steel. *Mater. Sci. Technol.* **8**, 1090–1094.

McLaren, A. J. & Sellars, C. M. 1993 The effects of transients in conditions of hot deformation on the kinetics of static recrystallisation. In *Proc. Int. Symp. on Strip Casting, Hot and Cold Working of Stainless Steels, Quebec* (ed. N. D. Ryan, A. J. Brown & H. J. McQueen), pp. 107–115. Quebec: Canadian Institute of Mining, Metallurgy and Petroleum.

Mukhopadhyay, A. 1998 Finite element modelling of hot rolling and local microstructure evolution. PhD thesis, The University of Sheffield, UK.

Pinna, C., Higginson, R. L. & Beynon, J. H. 1998 Uncertainties in modelling the evolution of crystallographic texture. Presented at *Modelling of Metal Rolling Process Symp. 9, December 1988.* Institute of Materials.

Ponter, A. R. S., Li, X. K. & Beynon, J. H. 1993 In *Proc. 1st Int. Conf. On Modelling of Metal Rolling Processes*, pp. 16–30. London: Institute of Materials.

Poths, R. 1998 The effects of strain history on the recrystallisation kinetics of copper. Final year project report, The University of Sheffield, UK.

Raabe, D. 1995*a* Microstructure and crystallographic texture of strip-cast and hot-rolled austenitic stainless-steel. *Metall Mater. Trans.* A **26**, 991–998.

Raabe, D. 1995*b* Inhomogeneity of the crystallographic texture in a hot-rolled autenitic stainless-steel. *J. Mater. Sci.* **30**, 47–52.

Rollett, A. D., Lowe, T., Kocks, U. K. & Stout, M. G. 1988 The microstructure and texture of torsion-reverse torsion experiments. In *Proc. 8th Int. Conf. on Textures of Materials (ICOTOM 8)* (ed. J. S. Kallend & G. Gottstein), pp. 473–478. Warrendale, PA: Met. Soc. AIME.

Sakai, T., Saito, Y. & Kato, K. 1987 Recrystallisation and texture formation in high speed hot rolling of austenitic strainless steel. *Trans. Iron Steel Inst. Jap.* **27**, 520–525.

Sellars, C. M. & Zhu, Q. 1998 Microstructural evolution during hot deformation of aluminium–magnesium alloys. In *Symp. on Hot Deformation of Aluminium Alloys II, TMS Fall Meeting, Chicago, October 1998*, pp. 185–197. Warrendale, PA: The Minerals, Metals and Materials Society.

Shrivistava, S. C., Jonas, J. J. & Canova, G. R. 1982 Equivalent strain in large deformation torsion testing—theoretical and practical considerations. *J. Mech. Phys. Solids* **30**, 75–90.

Stout, M. G. & Rollett, A. D. 1990 Large-strain Bauschinger effect in FCC metals and alloys. *Metall. Trans.* **21**, 3201–3212.

Takeshita, T., Kocks, U. F. & Wenk, H. 1988 The path dependence of deformation texture development. In *Proc. 8th Int. Conf. on Textures of Materials (ICOTOM 8)* (ed. J. S. Kallend & G. Gottstein), pp. 445–448. Warrendale, PA: Met. Soc. AIME.

Taylor, G. I. 1938 Plastic strain in metals. *J. Inst. Metals* **62**, 307–324.

Vatne, H. E., Mousavi, M. G., Benum, S., Rønning, B. & Nes, E. 1996 Texture and structure evolution in Al–Mn and commercial purity aluminium deformed by monotonic and reversed hot torsion. *Mater. Sci. Forum* **217–222**, 553–558.

Wang, C. H. & Brown, M. W. 1994 A study of the deformation-behaviour under multi-axial loading. *Eur. J. Mech.* A **13**, 175–188.

Zhang, X. J., Thompson, P. F. & Hodgson, P. D. 1997 The stress–strain and recrystallisation behaviour for deformation involving a change in strain path. In *Proc. Thermec 97 Int. Conf. on Thermomechanical Processing of Steels and Other Materials*, vol. II, pp. 1705–1711. Warrendale, PA: The Minerals, Metals and Materials Society.

Zhu, Q. & Sellars, C. M. 1996 Effect of deformation paths on static recrystallisation behaviour of an Al–2Mg alloy. In *Proc. 3rd Int. Conf. On Recrystallisation and Related Phenomena (ReX'96), California* (ed. T. R. McNelley), pp. 195–202. Monterey Institute of Advanced Studies.

Discussion

P. J. Withers (*Manchester Materials Science Centre, UK*). As Professor Sellars has shown, yield stress differences on changing strain path provide very little insight into changes in the microstructure. For example, the differences between the Mn-containing and Mn-free Al alloys he presented could be due to internal stresses developed in the former. I agree that other evidence (recrystallization kinetics, diffraction line broadening, etc.) may be more useful.

C. M. Sellars. The dislocation structure controls both the flow stress and the recrystallization behaviour. However, flow stress is a bulk property or depends primarily on the total dislocation density, whereas nucleation of recrystallization depends on local heterogeneities in dislocation structure, and so should be more sensitive to dislocation distribution. We therefore believe that both types of measurements should be made.

P. van Houtte (*Department MTM, K.U. Leuven, Belgium*). A statistical model would not be able to predict that after a strain path change, there may be a negative shape in the stress response. The presence of such a negative slope is vital in

simulations of sheet-metal operations. Indeed, they will trigger sudden failure of the sheet.

Any simulation of a sheet-metal-forming operation must be capable of predicting this if they should be of any use to industry at all.

C. M. Sellars. I agree, we are proposing that the statistically stored dislocations only lead to isotropic hardening and the geometrically necessary dislocations, which accommodate in-grain curvatures, are primarily responsible for strain-path effects.

L. M. Brown (*Cavendish Laboratories, University of Cambridge, UK*). Regarding the energy stored after cold work, the presence of undeformable particles not only produces a Bauschinger effect, but also a much enhanced stored energy, which promotes recrystallization.

C. M. Sellars. These comments are also true for hot work if the undeformable particles are sufficiently large. For the Al–Mg alloys studied in tension–tension and tension–compression (figure 8) the particles in the commercial-purity alloys were not large enough to cause particle-stimulated nucleation of recrystallization after the experimental deformation conditions.

P. Prangnell (*Manchester Materials Science Centre, UK*). Using equal channel angular extrusion with a reversed shear strain, preliminary results on Al–3%Mg tested at 200 °C have shown that even at very high total strains ($\gamma = 17$), few high misorientation boundaries are generated within the grains and the grain shape is largely reassembled. However, around the edge of the grains imperfections develop and new high-angle boundaries are formed.

PHILOSOPHICAL TRANSACTIONS OF THE ROYAL SOCIETY A MATHEMATICAL, PHYSICAL & ENGINEERING SCIENCES